Passive volumetric time domain simulation for room acoustics applications

Passive Volumetric Time Domain Simulation for Room Acoustics Applications

Stefan Bilbao[1] and Brian Hamilton[1]

Acoustics and Audio Group, Alison House, 12 Nicolson Square, University of Edinburgh, Edinburgh, EH8 9DF, United Kingdom[a)]

A major design consideration for volumetric wave-based time-domain room acoustics simulation methods, such as finite difference time domain (FDTD) methods, much be sufficiently general, or robust, to handle irregular room geometries and frequency-dependent and spatially varying wall conditions. A general framework for the design of such schemes is presented here, based on the use of the passivity concept which underpins realistic wall conditions. This analysis is based on the use of conservative finite volume methods, allowing for a representation of the room system as a feedback connection of a lossless part, corresponding to wave propagation over the interior, and a lossy subsystem, representing the effect of wall admittances. Such a representation includes simpler FDTD methods as a special case, and allows for the determination of stability conditions for a variety of time-stepping strategies.

 [http://dx.doi.org(DOI number)]

[XYZ] Pages: 1–13

The following article has been accepted for publication in the Journal of the Acoustical Society of America. After it is published, it will be found at `http://asa.scitation.org/journal/jas`

I. INTRODUCTION

Time-domain volumetric wave-based simulation is a general approach to the problem of room acoustics simulation for virtual acoustics and auralisation. In contrast with methods based on geometrical acoustics (such as ray tracing[1] or the image source method[2]), it naturally captures all features of wave propagation in an enclosure, including diffraction, and allows for a detailed treatment of the room boundary under very mild assumptions. The hallmark of volumetric wave-based simulation methods is a complete representation of the acoustic field over a grid covering the enclosure. Though computationally intensive, such methods are well-suited to parallel implementation [3,4], and recently it has become possible to generate output at audio rates for reasonably large acoustic volumes[5]. Time domain methods may be viewed in contrast to methods expressed directly in the frequency domain, such as the (non-volumetric) boundary element method[6].

Various methodologies have been proposed. The simplest, and best-suited to implementation in parallel hardware, are methods defined over regular grids such as finite difference time domain (FDTD) methods, which have long roots in mainstream simulation design, and particularly electromagnetic field simulation[7] and geophysics[8]. FDTD methods were proposed for use in low-frequency room acoustics problems in the 1990s[9–11], along with equivalent digital waveguide mesh methods[12,13]. There are many varieties[14,15], which differ chiefly in terms of computational cost and the ability to suppress perceptually-salient artefacts such as numerical dispersion[16]. A generalisation of FDTD methods to unstructured grids is the finite volume time domain method (FVTD); such methods allow for fine-grained modeling of irregular geometries[11,17,18], and the ability to model frequency-dependent and spatially-varying wall conditions directly, without resorting to operation over frequency bands[19]. FDTD and FVTD methods rely on local discretisations of the wave equation—non-local spectral methods[20,21] have also been proposed, allowing for increased accuracy over simple geometries such as box-shaped regions or concatenations of such regions[22].

A major concern in all time domain room acoustics simulation methods is the determination of conditions for numerical stability—it is especially difficult given a) the complexity of the typical room geometry, b) the nontrivial nature of the wall condition, including frequency dependence as well as spatial variation over the wall surface, c) the nearly lossless nature of the problem—additional damping is not present as a safeguard against explosive numerical solution growth, and d) the relatively long duration of simulations, which may in the millions of time steps. Indeed, without a solid guarantee of numerical stability, ad hoc methods are prone to numerical instability, manifesting itself as exponential solution growth, usually as a result of a poorly chosen numerical boundary condition. See Figure I. The aim of this article is to provide a general framework for the robust design of wave-based time domain simulation algorithms for room acoustics, under the most general conditions possible.

a)sbilbao@ed.ac.uk;

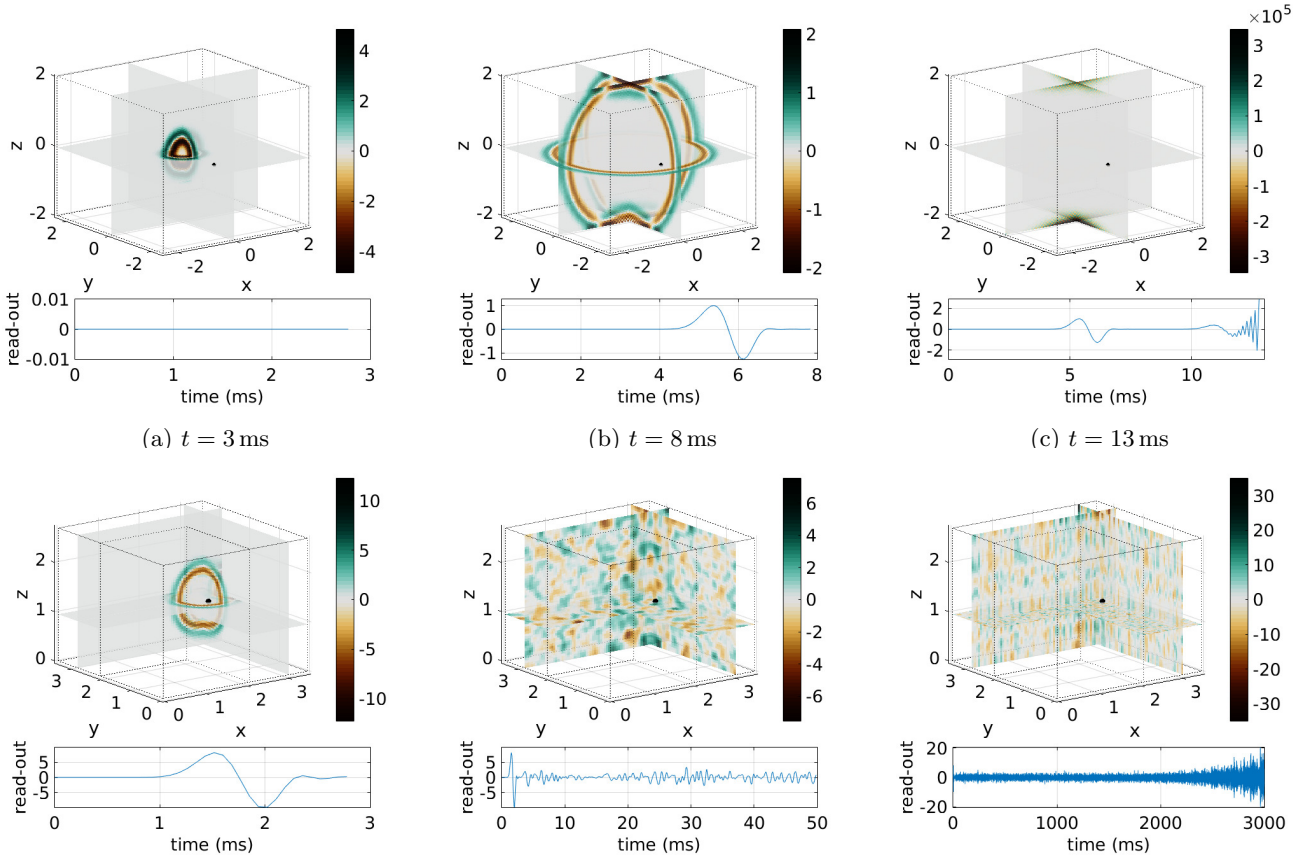

(a) $t = 3\,\mathrm{ms}$ (b) $t = 8\,\mathrm{ms}$ (c) $t = 13\,\mathrm{ms}$

(d) $t = 3\,\mathrm{ms}$ (e) $t = 50\,\mathrm{ms}$ (f) $t = 3\,\mathrm{s}$

FIG. 1. Illustrations of numerical instabilities at rigid domain boundaries due to unstable, yet consistent, numerical boundary conditions. Snapshots of wave propagation are shown at times indicated, and the read-out position is denoted by a black sphere. In the top row, the walls of the box-shaped room are truncated as described in Ref. 23, which is known to be unstable. In bottom row, the L-shaped room has an improper corner condition causing a slow instability, as reported in Refs. 15,24,25.

A typical approach to the determination of numerical stability conditions, for FDTD methods defined over regular grids is through von Neumann analysis[26]. This is a combination of discrete spatial Fourier transform and z-transform analysis, applied generally in the absence of boundary conditions (i.e., for an infinite or spatially periodic domain). Such techniques are simply applied, but for problems defined over a finite region are limited to yielding necessary but not sufficient conditions for stability. Extensions to arrive at stability conditions for simple bounded regions, such as half or quarter spaces have been proposed some time ago by various authors [27–29], and similar methods were used later in general acoustics[30,31] and room acoustics applications[14], incorporating immittance boundary conditions. Such a methodology, based fundamentally on properties of Fourier transforms as applied to shift-invariant systems, does not extend easily to the case of spatially-varying wall conditions or irregular geometries, cases typically seen in real-world room acoustics problems.

A different approach is through so-called energy techniques. The rate of growth of the numerical solution generated by a time-stepping method may be bounded in terms of an non-negative, energy-like function. In particular, if wall admittances are passive (that is, wall materials are able to store or dissipate energy, but not produce it), then it is possible to design a numerical simulation method to mimic this property in discrete time, leading to a stable simulation design[17,18]. Such a methodology is directly related to geometric numerical integration techniques[32]. This direct time-domain approach to stability analysis relies on the availability of a concrete realisation for a given wall admittance—one must have precise knowledge of the loss and energy storage mechanisms corresponding to a given admittance. This can become difficult if, as is the case in practice, the admittance is only known through relatively coarse measurements and a model of the admittance mechanism itself is unknown.

The passivity property is encapsulated by the combination of a lossless system (the room interior) and a combination of losses and additional energy storage at the room boundary or wall. For linear and time-invariant systems such as room acoustics under static conditions, passivity follows from the positive real property of admittances in the frequency domain. This leads to a more simple and general approach to stability analysis, which is independent of any particular realisation of the wall admittance itself, and which extends to a variety of well-known time-stepping methods in discrete time. It is this

more general framework that will be illustrated in this article.

The basic energetic properties of the room acoustics system are described in Section II with regard to the very simple test problem of the oscillator under a general passive damping law, characterised by a positive real admittance. A general model of room acoustics, for arbitrary geometries, and under arbitrary passive wall impedance conditions is presented in Section III, followed by a reformulation in semi-discrete form, through finite volume methods, in Section IV, where wall losses are introduced as an additional feedback term, again positive real, in analogy to the case of the oscillator. Fully discrete numerical schemes, of explicit and implicit type, are presented in Section V accompanied by implementation details as well as sufficient stability conditions, deduced through the enforcement of the positive realness property. Preliminary results from this article have appeared in a recent proceedings paper[33].

II. THE MASS-SPRING SYSTEM

Many important features of room acoustics modeling can be seen, in miniature, in the very simple test problem of a simple mass-spring system under a connection to a further passive subnetwork, of perhaps unknown internal structure, and leading to frequency-dependent damping.

The defining equations of a lossless lumped mass spring system may be written as

$$M\frac{dv}{dt} - f = 0 \qquad \frac{1}{K}\frac{df}{dt} + v = 0 \quad . \tag{1}$$

The velocity $v(t)$ in $\mathrm{m{\cdot}s^{-1}}$ and force $f(t)$ in N are both functions of time $t \in [0, \infty)$ in s. The first equation can be identified with Newton's second law and the second with the constitutive law of a linear spring. The mass M in kg and stiffness K in $\mathrm{kg{\cdot}\ s^{-2}}$ are both strictly positive.

As a preliminary step, it is useful to introduce the scaled variables $\tilde{v}$ and $\tilde{f}$, defined as

$$\tilde{v} = \sqrt{M}v \qquad \tilde{f} = f/\sqrt{K} \quad , \tag{2}$$

with units of root energy. After insertion in (1) and the removal of the tilde notation, the scaled system

$$\frac{dv}{dt} - \omega_0 f = 0 \qquad \frac{df}{dt} + \omega_0 v = 0 \tag{3}$$

results, where $\omega_0 = \sqrt{K/M} > 0$.

Under a two-sided Laplace transformation defined, for a function $g(t)$, as

$$\hat{g}(s) = \int_{-\infty}^{\infty} g(t)\, e^{-st} dt \tag{4}$$

for complex frequencies s, system (3) may be written as

$$\underbrace{\begin{bmatrix} s & \omega_0 \\ -\omega_0 & s \end{bmatrix}}_{\mathbf{G}(s)} \begin{bmatrix} \hat{f} \\ \hat{v} \end{bmatrix} = \begin{bmatrix} 0 \\ 0 \end{bmatrix} \quad . \tag{5}$$

Nontrivial solutions follow for values of s for which $\det(\mathbf{G}(s)) = 0$, leading immediately to

$$s = \pm j\omega_0 \quad . \tag{6}$$

The general solution to (3) is thus sinusoidal, of frequency ω_0, reflecting losslessness of the underlying system.

As a simpler alternative to Laplace transformation, one may examine test solutions of the form

$$f = \hat{f}e^{st} \qquad v = \hat{v}e^{st} \tag{7}$$

for complex amplitudes $\hat{f} = \hat{f}(s)$ and $\hat{v} = \hat{v}(s)$, leading to the same conclusions above. This abbreviated analytical approach will be taken remainder of this article.

A. A Loss Term

Consider now an extension to the scaled system (3):

$$\frac{dv}{dt} - \omega_0 f = 0 \qquad \frac{df}{dt} + \omega_0 v + \omega_0 v' = 0 \quad , \tag{8}$$

where v', which also has dimensions of root energy, is defined in terms of f via the differential relationship:

$$\sum_{\nu=0}^{M} \xi^{(\nu)} \frac{d^\nu v'}{dt^\nu} = \sum_{\nu=0}^{D} \eta^{(\nu)} \frac{d^\nu f}{dt^\nu} \quad , \tag{9}$$

for some constants $\xi^{(\nu)}$, $\nu = 0, \ldots, M$ and $\eta^{(\nu)}$, $\nu = 0, \ldots, D$. $\xi^{(M)}$ and $\eta^{(D)}$ are assumed non-zero.

System (8) has an electrical network representation, through association of v and v' with currents, and f with voltage. See Figure 2. The general form is of a lossless network corresponding to system (3) coupled to a subnetwork representing losses, the internal behaviour of which is described by (9). The analogy with room acoustics follows from an association of the lossless system with the wave equation over the room interior, and the lossy subnetwork with wall dissipation. See Section IV.

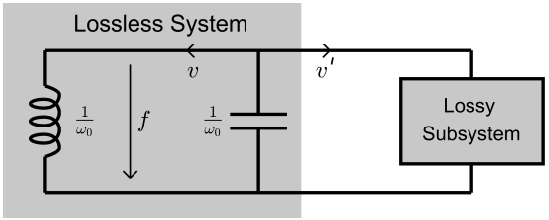

FIG. 2. Network representation of system (8).

Using (7) in addition to $v' = \hat{v}'e^{st}$, (9) becomes

$$\hat{v}' = Y(s)\,\hat{f} \quad \text{where} \quad Y(s) = \frac{\sum_{\nu=0}^{D} \eta^{(\nu)} s^\nu}{\sum_{\nu=0}^{M} \xi^{(\nu)} s^\nu} \quad . \tag{10}$$

$Y(s)$ can be interpreted as a nondimensional admittance.

The following system results:

$$\underbrace{\begin{bmatrix} s + \omega_0 Y(s) & \omega_0 \\ -\omega_0 & s \end{bmatrix}}_{\mathbf{G}(s)} \begin{bmatrix} \hat{f} \\ \hat{v} \end{bmatrix} = \begin{bmatrix} 0 \\ 0 \end{bmatrix} \quad , \tag{11}$$

and as before, nontrivial solutions result for values $s = \bar{s}$ for which $\det(\mathbf{G}(\bar{s})) = 0$. At this point, it is of interest to find conditions on $Y(s)$ which are sufficient to ensure that any frequency $\bar{s}$ satisfies $\mathrm{Re}(\bar{s}) \leq 0$, and thus from the *ansatz* (7) exponential solution growth is ruled out. While for this simple test problem it is possible to numerically solve for the solutions to $\det(\mathbf{G}(s)) = 0$, the judicious use of the concept of passivity and positive realness of an admittance function leads to a greatly simplified analysis which extends to the much more involved case of room acoustics simulation. See Section III.

B. Positive Realness and Passivity

In order to represent a mechanism capable of dissipating energy, the function $Y(s)$ must be positive real—a well-known result from electrical network theory[34]. The concept of positive realness has also been employed in a simulation setting, both in the case of electrical circuit networks through wave digital filters[35], as well as in the modeling of musical instruments—see recent work on numerical modeling of losses in acoustic tubes[36] and strings[37].

While there are various definitions of positive realness which differ slightly, we will take the following definition[38], which is applicable to complex functions of rational form such as $Y(s)$ as defined in (10).

$$\mathrm{Re}(Y(s)) \geq 0 \qquad \text{when} \qquad \mathrm{Re}(s) > 0 \quad . \tag{12}$$

In addition, $Y(s)$ must satisfy the condition that it takes on real values for real values of its argument. The positive realness condition imposes restrictions on the form of a rational function. For example, a necessary but not sufficient condition is that all poles and zeros lie in the left half plane; another is that the orders of the numerator and denominator polynomials of $Y(s)$ may differ by at most 1. For a given rational positive real function, various synthesis procedures exist[34], leading to concrete realisations in terms of canonical energy-storing or dissipating units. But the precise realisation is immaterial in a simulation setting—all that is needed is the basic positive realness property defined above.

Returning now to the condition $\det(\mathbf{G}(s)) = 0$, suppose that a solution $\bar{s}$ exists such that $\mathrm{Re}(\bar{s}) > 0$. One may write $\det(\mathbf{G}(\bar{s})) = G_{22}(\bar{s})\, G_{22}^{SC}(\bar{s})$, where

$$G_{22}(\bar{s}) = \bar{s} \qquad G_{22}^{SC}(\bar{s}) = \bar{s} + \omega_0 Y(\bar{s}) + \omega_0^2/\bar{s} \quad . \tag{13}$$

Here, $G_{22} \neq 0$ is the bottom right entry of $\mathbf{G}$, and G_{22}^{SC} is its Schur complement[39]. Clearly $G_{22}^{SC}(\bar{s})$ must vanish. Taking the real part of $G_{22}^{SC}(\bar{s})$, and using $\bar{s} = \bar{\sigma} + j\bar{\omega}$, with $\bar{\sigma} > 0$, one has, immediately,

$$\mathrm{Re}(G_{22}(\bar{s})) = \bar{\sigma} + \omega_0 \mathrm{Re}(Y(\bar{s})) + \frac{\omega_0^2 \bar{\sigma}}{\bar{\sigma}^2 + \bar{\omega}^2} \quad . \tag{14}$$

From the positive realness property (12), all terms are either positive or non-negative for $\bar{\sigma} = \mathrm{Re}(\bar{s}) > 0$ and neither of the two factors of the determinant can vanish. All solutions $\bar{s}$ must have $\bar{\sigma} \leq 0$, and thus there is no solution to system (8) which exhibits exponential growth.

C. Comment

The result above is intuitively obvious given the representation in Figure 2—this is a network consisting of passive elements, and thus dissipative as a whole. The subdivision of the system into a primary lossless part and a more complex loss mechanism is a good starting point for numerical design, especially when the effect of the loss mechanism in the system as a whole is relatively small. This is precisely the case in room acoustics, where the room geometry determines dominant features such as modal frequencies and echo times and densities, and the wall conditions lead mainly to a long-term energy decay of a complex character, with some possible adjustment of mode frequencies. Often, simple and efficient numerical methods exist for the primary lossless part of the system (in room acoustics, the wave equation), and it is profitable to be able to use such designs directly in conjunction with much more complex methods required to model realistic wall conditions, without additional concerns due to interactions leading potentially to numerical instability. As will be outlined subsequently, the positive realness property of wall admittances can be used in order to generate guaranteed stable numerical designs.

III. ROOM ACOUSTICS MODELING

The usual starting point for room acoustics modeling is the following system of equations:

$$\frac{1}{\rho c^2}\partial_t p + \nabla \cdot \mathbf{v} = 0 \tag{15a}$$

$$\rho \partial_t \mathbf{v} + \nabla p = \mathbf{0} \quad . \tag{15b}$$

Here, the field variables $p(\mathbf{x}, t)$ and $\mathbf{v}(\mathbf{x}, t)$ are the acoustic pressure and vector particle velocity, respectively. Both are defined for coordinates $\mathbf{x} \in \mathcal{D} \subset \mathbb{R}^3$, where $\mathcal{D}$ represents the region over which the problem is defined (the room interior) and for time $t \in \mathbb{R}$. ρ and c are air density in kg$\cdot$ m^{-3} and wave speed in m$\cdot$ s^{-1}, respectively. ∂_t represents partial differentiation with respect to time t, and ∇ and $\nabla\cdot$ are the three dimensional gradient and divergence operations, respectively. The system (15) generalises the oscillator system given in (1). It is defined here for all time, allowing the same analysis approach as in the case of the lumped oscillator in Section II. For a system defined over $t \in [0, \infty)$, two initial conditions, $p(\mathbf{x}, 0)$ and $\mathbf{v}(\mathbf{x}, 0)$ must be supplied.

The system (15) can be reduced to the second order wave equation in p alone:

$$\partial_t^2 p - c^2 \Delta p = 0 \tag{16}$$

where the Laplacian Δ is defined as $\Delta = \nabla \cdot \nabla$. In the remainder of this article the first order system (15) will be employed. See, however, the remarks at the end of Section V B.

A. Locally Reactive Boundary Conditions

To complete system (15), a single boundary condition must be supplied at each point $\mathbf{x} \in \partial\mathcal{D}$, where $\partial\mathcal{D}$

is the boundary of the domain $\mathcal{D}$. Locally reactive conditions can be expressed as a pointwise relationship between the pressure $p(\mathbf{x},t)$ and the outward normal velocity $v_{\mathbf{n}}(\mathbf{x},t) = \mathbf{n}\cdot\mathbf{v}(\mathbf{x},t)$, at points $\mathbf{x}\in\partial\mathcal{D}$, where $\mathbf{n}$ is the outward normal vector to the boundary at $\mathbf{x}$.

The condition is usually expressed in the frequency domain through an admittance. Following the approach used in the case of the oscillator in Section II, one may examine time-exponential solutions of the form $p(\mathbf{x},t) = e^{st}\hat{p}(\mathbf{x},s)$ and $\mathbf{v}(\mathbf{x},t) = e^{st}\hat{\mathbf{v}}(\mathbf{x},s)$. A locally-reactive admittance boundary condition may be expressed as

$$\hat{v}_{\mathbf{n}} = Y(\mathbf{x},s)\,\hat{p} \tag{17}$$

for $\mathbf{x}\in\partial\mathcal{D}$. Y may vary from one location to another over the room boundary $\partial\mathcal{D}$ as is natural in a realistic room acoustics setting. In order to represent a passive wall condition, the admittance is constrained to be positive real, as per the definition (12), for all $\mathbf{x}\in\partial\mathcal{D}$.

IV. SEMI-DISCRETE MODELS

Before proceeding to a fully discrete simulation algorithm, a useful intermediate step is semidiscretisation over a spatial grid or lattice. There are obviously many approaches to this, including finite difference and finite element methods. A useful technique, which allows for specialisation to well-known finite difference discretisations commonly used in wave-based acoustics models, is the finite volume method, which has been described in previous works[17,18]. It has the advantage of allowing for local updates over the bulk of the room volume, but for specialisation to irregular boundary surfaces. Stability analysis is simplified due to the conservative nature of the finite volume formalism, as illustrated below.

A. Cells and Adjacency

The domain $\mathcal{D}$ is assumed decomposed into N non-overlapping polyhedra, or cells Ω_l, $l=1,\ldots,N$, of volume $V_l = |\Omega_l|$. The set of such polyhedra will possess N_e internal faces $\mathcal{S}_e$ joining two adjacent cells, and let the area of such an internal face be written as $S_e = |\mathcal{S}_e|$, $e=1,\ldots,N_e$. Also associated with internal face e is an inter-cell distance H_e, $e=1,\ldots,N_e$. There will be N_b unadjoined exterior or boundary faces $\mathcal{R}_b$ located on the boundary $\partial\mathcal{D}$ of $\mathcal{D}$—the areas of these boundary faces are $R_b = |\mathcal{R}_b|$, $b=1\ldots,N_b$. See Figure 3.

A given face e is adjacent to two cells of index l_e^+ and l_e^- where $l_e^+ > l_e^-$. One may define an oriented adjacency 2-tensor $Q_{l,e}$, where $l=1,\ldots,N$ and $e=1,\ldots,N_e$, as

$$Q_{l,e} = \begin{cases} 1 & \text{if } l = l_e^+ \\ -1 & \text{if } l = l_e^- \\ 0 & \text{otherwise} \end{cases} . \tag{18}$$

Similarly, for a boundary face $\mathcal{S}_b'$, adjacent to exactly one cell with $l=l_b$, one may define a non-oriented adjacency

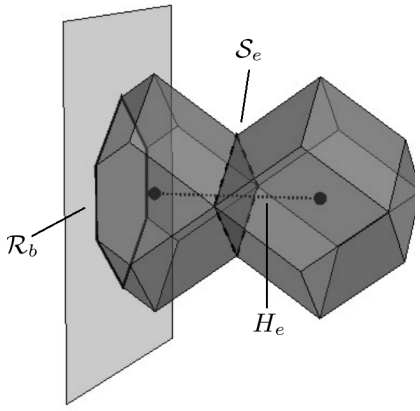

FIG. 3. Illustration of two adjacent finite volume cells. Here, the internal face $\mathcal{S}_e$ is outlined with dashed lines, the inter-cell distance H_e is denoted by a dotted line, and the boundary face $\mathcal{R}_b$ is outlined in thick black line. Here, the inter-cell distance is chosen such that the face adjoining the two adjacents cells divides evenly, and is perpendicular to, the line segment that defines H_e.

tensor $W_{l,b}$, $l=1,\ldots,N$ and $b=1,\ldots,N_b$ as

$$W_{l,b} = \begin{cases} 1 & \text{if } l = l_b \\ 0 & \text{otherwise} \end{cases} . \tag{19}$$

For room acoustics simulation, and at an audio rate such as 48 kHz, the average linear dimension of a cell must be chosen on the order of approximately 1 cm (which is roughly half the shortest audible wavelength), and thus the problem size, characterised by the number of cells N, will be very large. For the sake of increased computational efficiency through parallelisation techniques, a structured arrangement of cells, such as cubes, over the problem interior can be complemented by an irregular tiling, fitted to the room boundary. See Figure 4, illustrating different possible arrangements. Finite volume methods over regular arrangements of cells reduce to well-known finite difference time domain methods[18].

B. A Finite Volume Method

The procedure for developing a finite volume method begins from the integration of (15a) over the cell Ω_l:

$$\frac{1}{\rho c^2}\iiint_{\Omega_l}\partial_t p\,d\mathbf{x} + \iiint_{\Omega_l}\nabla\cdot\mathbf{v}\,d\mathbf{x} = 0 . \tag{20}$$

For the first term above, one may use the following definition of the averaged cell pressure $p_l = p_l(t)$ for cell Ω_l:

$$p_l \triangleq \frac{1}{V_l}\iiint_{\Omega_l} p\,d\mathbf{x} . \tag{21}$$

For the second term, one may employ the divergence theorem to yield

$$\iiint_{\partial\Omega_l}\nabla\cdot\mathbf{v}\,d\mathbf{x} = \iint_{\partial\Omega_l}\mathbf{n}\cdot\mathbf{v}\,d\sigma , \tag{22}$$

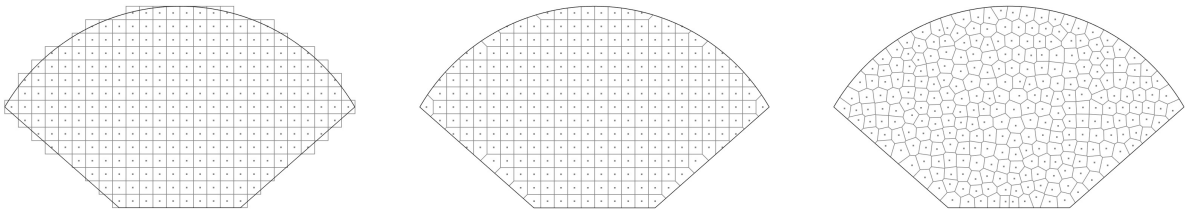

FIG. 4. Illustrations of different arrangements of finite volume cells, in two dimensions for purposes of demonstration. Here, the fan-shaped room is represented by (left): a staircased, regular Cartesian mesh; (center): an irregular Cartesian mesh, where cells are fitted to the domain near the boundaries; and (right): an fully-unstructured fitted mesh.

where $\partial\Omega_l$ is the boundary of the cell Ω_l, and where $\mathbf{n}$ represents its outward normal. This surface integral may then be decomposed into contributions over the adjoining faces (including those which lie on the boundary of the room volume $\mathcal{D}$). Employing the definitions of the adjacency tensors Q and W from (18) and (19),

$$\iiint_{\partial\Omega_l} \nabla\cdot\mathbf{v}\, d\mathbf{x} \approxeq -\sum_{e=1}^{N_e} Q_{l,e} S_e v_e + \sum_{b=1}^{N_b} W_{l,b} R_b v'_b \quad . \tag{23}$$

Here, $v_e = v_e(t)$ represents the average component of the velocity normal to the face $\mathcal{S}_e$, and oriented in the direction from $\Omega_{l_e^-}$ to $\Omega_{l_e^+}$. Similarly, $v'_b = v'_b(t)$ is the scalar component of the velocity normal to the boundary, averaged over boundary face $\mathcal{R}_b$, and oriented outward.

Equation (15b) may be approximated, for a given velocity component v_e, through an approximation to the normal gradient of the pressure between the cells adjacent to the edge (assumed separated by a distance H_e), again employing the adjacency tensor $Q_{l,e}$. The resulting approximation to system (15) may then be written, in terms of scalar pressures p_l, $l = 1,\ldots,N$ and velocities v_e, $e = 1,\ldots,N_e$ and v'_b, $b = 1,\ldots,N_b$ as

$$\frac{V_l}{\rho c^2}\frac{dp_l}{dt} - \sum_{e=1}^{N_e} Q_{l,e} S_e v_e + \sum_{b=1}^{N_b} W_{l,b} R_b v'_b = 0 \tag{24a}$$

$$\rho H_e \frac{dv_e}{dt} + \sum_{l=1}^{N} Q_{l,e} p_l = 0 \quad . \tag{24b}$$

C. Wall Conditions

The boundary velocity components v'_b, $b = 1,\ldots,N_b$ in (24) remain as yet unspecified. It is clear that the locally reactive property of wall admittances implies that, in the semi-discrete setting, the outward normal velocity v'_b should be related to the pressure in the unique adjoining cell p'_b. In analogy with the case of the oscillator, consider a general differential relationship of the form

$$\sum_{\nu=0}^{M_b} \xi_b^{(\nu)} \frac{d^\nu v'_b}{dt^\nu} = \frac{1}{\rho c}\sum_{\nu=0}^{D_b} \eta_b^{(\nu)} \frac{d^\nu p'_b}{dt^\nu} \quad , \tag{25}$$

for some constants $\xi_b^{(\nu)}$, $\nu = 0,\ldots,M_b$ and $\eta_b^{(\nu)}$, $\nu = 0,\ldots,D_b$ and $b = 1,\ldots,N_b$. The relationship above is dependent on the particular boundary face and the resulting admittance is thus variable over the wall. The adjoining cell pressure p'_b for boundary face b can be retrieved from the set of cell pressures p_l, $l = 1,\ldots,N$ through the adjacency tensor W as

$$p'_b = \sum_{l'=1}^{N_b} W_{l',b} p_{l'} \quad . \tag{26}$$

D. Vector-matrix Form and Scaling

The equations (24), (25) and (26) form a complete system of ordinary differential equations for the room acoustics problem. For analysis purposes, it is useful to rewrite it in vector-matrix form. To this end, defining the column vectors $\mathbf{p} = [p_1,\ldots,p_N]^T$, $\mathbf{v} = [v_1,\ldots,v_{N_e}]^T$, $\mathbf{v}' = [v'_1,\ldots,v'_{N_b}]^T$ and $\mathbf{p}' = [p'_1,\ldots,p'_{N_b}]^T$, one then has

$$\frac{1}{\rho c^2}\mathbf{V}\frac{d}{dt}\mathbf{p} - \mathbf{QSv} + \mathbf{WRv}' = \mathbf{0} \tag{27a}$$

$$\rho\mathbf{H}\frac{d}{dt}\mathbf{v} + \mathbf{Q}^T\mathbf{p} = \mathbf{0} \quad , \tag{27b}$$

accompanied by the auxiliary boundary system

$$\sum_{\nu=0}^{M_b} \xi_b^{(\nu)} \frac{d^\nu v'_b}{dt^\nu} = \frac{1}{\rho c}\sum_{\nu=0}^{D_b} \eta_b^{(\nu)} \frac{d^\nu p'_b}{dt^\nu} \qquad \mathbf{p}' = \mathbf{W}^T\mathbf{p} \quad . \tag{28}$$

Here, $\mathbf{V}$ is an $N\times N$ diagonal matrix with the cell volumes V_l, $l = 1,\ldots,N$ on the diagonal, and similarly, $\mathbf{S}$ and $\mathbf{H}$ are $N_e\times N_e$ diagonal matrices with S_e and H_e on their diagonals, respectively, $e = 1,\ldots,N_e$. $\mathbf{R}$ is a diagonal matrix with R_b on the diagonal, for $b = 1,\ldots,N_b$. The matrices $\mathbf{Q}$ and $\mathbf{W}$ are the matrix forms of the adjacency tensors Q and W, as defined in (18) and (19), and are of size $N\times N_e$ and $N\times N_b$, respectively.

E. Scaling

Introduce the scaled variables $\tilde{\mathbf{p}}$ and $\tilde{\mathbf{v}}$ (with units of root energy), as

$$\tilde{\mathbf{p}} = \frac{1}{\sqrt{\rho c}}\mathbf{V}^{\frac{1}{2}}\mathbf{p} \qquad \tilde{\mathbf{v}} = \sqrt{\rho}\mathbf{S}^{\frac{1}{2}}\mathbf{H}^{\frac{1}{2}}\mathbf{v} \quad . \tag{29}$$

(Here, $\mathbf{A}^{\frac{1}{2}}$ indicates the unique positive diagonal square root of the positive diagonal matrix $\mathbf{A}$.) Introduce as well the scaled boundary variables

$$\tilde{\mathbf{p}}' = \frac{1}{\sqrt{\rho c}}\mathbf{R}^{\frac{1}{2}}\mathbf{p}' \qquad \tilde{\mathbf{v}}' = \sqrt{\rho}\mathbf{R}^{\frac{1}{2}}\mathbf{v}' \quad . \tag{30}$$

After removing the tilde notation, the scaled system

$$\frac{d}{dt}\mathbf{p} - c\mathbf{D}^T\mathbf{v} + c\mathbf{B}^T\mathbf{v}' = \mathbf{0} \tag{31a}$$

$$\frac{d}{dt}\mathbf{v} + c\mathbf{D}\mathbf{p} = \mathbf{0} \tag{31b}$$

results, accompanied by the auxiliary relations

$$\sum_{\nu=0}^{M_b} \xi_b^{(\nu)} \frac{d^\nu v_b'}{dt^\nu} = \sum_{\nu=0}^{D_b} \eta_b^{(\nu)} \frac{d^\nu p_b'}{dt^\nu} \qquad \mathbf{p}' = \mathbf{B}\mathbf{p} \quad , \tag{32}$$

The matrices $\mathbf{D}$ and $\mathbf{B}$ are defined as

$$\mathbf{D} = \mathbf{S}^{\frac{1}{2}}\mathbf{H}^{-\frac{1}{2}}\mathbf{Q}^T\mathbf{V}^{-\frac{1}{2}} \qquad \mathbf{B} = \mathbf{R}^{\frac{1}{2}}\mathbf{W}^T\mathbf{V}^{-\frac{1}{2}} \quad , \tag{33}$$

where $\mathbf{D}$ approximates the 3D gradient operation. This scaled system will be used henceforth in this article.

F. Frequency Domain Representation

Similarly to the case of the oscillator in Section II, one may make use of the *ansatz* $\mathbf{w} = \hat{\mathbf{w}}e^{st}$, where $\mathbf{w}$ is any of the variables $\mathbf{p}$, $\mathbf{v}$, $\mathbf{p}'$ or $\mathbf{v}'$.

Consider first the boundary condition (32). The frequency domain representation is

$$\hat{\mathbf{v}}' = \mathbf{Y}\hat{\mathbf{p}}' \quad , \tag{34}$$

where $\mathbf{Y}(s)$ is an $N_b \times N_b$ diagonal matrix, with $Y_b(s)$ on the diagonal, $b = 1, \ldots, N_b$, where

$$Y_b(s) = \frac{\sum_{\nu=0}^{D_b} \eta_b^{(\nu)} s^\nu}{\sum_{\nu=0}^{M_b} \xi_b^{(\nu)} s^\nu} \quad . \tag{35}$$

For passivity, the rational functions $Y_b(s)$ are constrained here to be positive real, and represent the nondimensional wall admittance at boundary face b, $b = 1, \ldots, N_b$.

The full system (31)-(32) may be written in the frequency domain, after the elimination of $\hat{\mathbf{p}}'$ and $\hat{\mathbf{v}}'$, as

$$\underbrace{\begin{bmatrix} s\mathbf{I}_N + c\mathbf{B}^T\mathbf{Y}\mathbf{B} & -c\mathbf{D}^T \\ c\mathbf{D} & s\mathbf{I}_{N_e} \end{bmatrix}}_{\mathbf{G}(s)} \begin{bmatrix} \hat{\mathbf{p}} \\ \hat{\mathbf{v}} \end{bmatrix} = \begin{bmatrix} \mathbf{0} \\ \mathbf{0} \end{bmatrix} \quad . \tag{36}$$

Here, $\mathbf{I}_N$ and $\mathbf{I}_{N_e}$ are identity matrices of size $N \times N$ and $N_e \times N_e$, respectively.

G. Bounds on Pole Locations

In analogy with the case of the oscillator, nontrivial solutions to the system (36) will occur at frequencies $s = \bar{s}$ such that $\det(\mathbf{G}(\bar{s})) = 0$. Again, assume a solution $\bar{s} = \bar{\sigma} + j\bar{\omega}$ for which $\bar{\sigma} > 0$. From (36), one may write, using an expression for the determinant of a block matrix,

$$\det(\mathbf{G}(\bar{s})) = \det(\mathbf{G}_{22}) \det\left(\mathbf{G}_{22}^{SC}\right) \quad , \tag{37}$$

where

$$\mathbf{G}_{22} = \bar{s}\mathbf{I}_{N_e} \qquad \mathbf{G}_{22}^{SC} = \bar{s}\mathbf{I}_N + c\mathbf{B}^T\mathbf{Y}\mathbf{B} + \frac{c^2}{\bar{s}}\mathbf{D}^T\mathbf{D} \tag{38}$$

are the lower right-hand $N_e \times N_e$ block of $\mathbf{G}$, and its Schur complement, respectively. Clearly $\det(\mathbf{G}_{22}) = \bar{s}^{N_e} \neq 0$. This implies that we must have $\det\left(\mathbf{G}_{22}^{SC}\right) = 0$, which implies, further, that there must exist some column vector $\mathbf{x} \in \mathbb{C}^N$ with $\mathbf{x} \neq \mathbf{0}$, such that $\mathbf{x}^*\mathbf{G}_{22}^{SC}\mathbf{x} = 0$, and where $\mathbf{x}^*$ is the conjugate transpose of $\mathbf{x}$. But, taking the real part of $\mathbf{x}^*\mathbf{G}_{22}^{SC}\mathbf{x}$, and defining $\mathbf{w} = \mathbf{B}\mathbf{x}$, yields

$$\mathrm{Re}\left(\mathbf{x}^*\mathbf{G}_{22}^{SC}\mathbf{x}\right) = \underbrace{\bar{\sigma}|\mathbf{x}|^2}_{>0} + \underbrace{c\sum_{b=0}^{N_b} |w_b|^2 \mathrm{Re}\left(Y_b(\bar{s})\right)}_{\geq 0} + \underbrace{\frac{c^2\bar{\sigma}}{\bar{\sigma}^2 + \bar{\omega}^2}|\mathbf{D}\mathbf{x}|^2}_{\geq 0} > 0 \quad , \tag{39}$$

where the positive realness of Y_b, $b = 1, \ldots, N_b$ has been employed. Thus $\det\left(\mathbf{G}_{22}^{SC}(\bar{s})\right) \neq 0$, and furthermore $\det(\mathbf{G}(\bar{s})) \neq 0$, and one may conclude that there is no solution $\bar{s}$ to the system (36) with $\bar{\sigma} > 0$.

V. DISCRETE-TIME MODELS

A. Time Series and Discrete Time Operators

Consider now the simulation of system (31), accompanied by (32) in discrete time, with time step k in s (corresponding, in audio applications, to a sample rate of $F_s = 1/k$ Hz). A time series $\mathbf{w}^n$, indexed by integer n, represents an approximation to a continuously variable function $\mathbf{w}(t)$, at times $t = nk$. Here, $\mathbf{w}$ could represent an approximation to any of the vectors $\mathbf{p}$, $\mathbf{v}$, $\mathbf{p}'$ or $\mathbf{v}'$ which appear in system (31)-(32).

The shift operators e_+ and e_- are defined, in terms of their action on a time series $\mathbf{w}^n$ as

$$e_+\mathbf{w}^n = \mathbf{w}^{n+1} \qquad e_-\mathbf{w}^n = \mathbf{w}^{n-1} \quad . \tag{40}$$

Forward and backward difference operations δ_+ and δ_-, approximating a time derivative, can then be defined as

$$\delta_+ = \frac{1}{k}(e_+ - 1) \qquad \delta_- = \frac{1}{k}(1 - e_-) \quad , \tag{41}$$

and averaging operators μ_+ and μ_- as

$$\mu_+ = \frac{1}{2}(e_+ + 1) \qquad \mu_- = \frac{1}{2}(1 + e_-) \quad . \tag{42}$$

A useful further approximation to the time derivative is the operator $\delta_\circ$, defined as

$$\delta_\circ = (\mu_+)^{-1}\delta_+ \quad . \tag{43}$$

The inverse operation may be interpreted, in terms of two time series $\mathbf{f}^n$ and $\mathbf{g}^n$, as

$$\delta_\circ \mathbf{f} = \mathbf{g} \quad \Rightarrow \quad \delta_+\mathbf{f} = \mu_+\mathbf{g} \quad . \tag{44}$$

The operator $\delta_\circ$, for linear systems, has the interpretation of the trapezoid or midpoint rule.

For certain schemes, it is useful to view time series as being mutually interleaved; for example, for the explicit designs described in Section V B, the variables $\mathbf{p}^n$ and $\mathbf{v}^{n+\frac{1}{2}}$ represent time-interleaved approximations to $\mathbf{p}(t)$ and $\mathbf{v}(t)$ at $t = nk$ and $t = \left(n+\frac{1}{2}\right)k$, respectively. The half-index notation, which is standard in the electromagnetic simulation literature[7], is intended to be helpful, both in analysis and implementation, but does not indicate operation at a twice-oversampled rate.

B. Numerical Schemes

Consider first the auxiliary relations (32), defining the numerical admittance boundary conditions. The variables $\mathbf{p}'$, $\mathbf{p}$ and $\mathbf{v}'$ are to be approximated by time series $(\mathbf{p}')^n$, $\mathbf{p}^n$ and $(\mathbf{v}')^n$, respectively, for integer n. Assume furthermore that these relations are discretised, uniformly, using $d/dt \to \delta_\circ$. This leads to:

$$\sum_{\nu=0}^{M_b} \xi_b^{(\nu)} \delta_\circ^\nu \left(v_b'\right)^n = \sum_{\nu=0}^{D_b} \eta_b^{(\nu)} \delta_\circ^\nu \left(p_b'\right)^n \qquad (\mathbf{p}')^n = \mathbf{B}\mathbf{p}^n \tag{45}$$

where $\delta_\circ^\nu$ indicates a ν-fold composition of the operator $\delta_\circ$. Under this choice, the passive nature of the admittance boundary condition is preserved. See Section V E.

For the primary part of the semidiscrete system (31), representing wave propagation over the room interior, various choices are available. One simple choice is to make uniform use again of the operator $\delta_\circ$, leading to the discrete time system:

$$\delta_\circ \mathbf{p}^n - c\mathbf{D}^T \mathbf{v}^n + c\mathbf{B}^T (\mathbf{v}')^n = \mathbf{0} \tag{46a}$$

$$\delta_\circ \mathbf{v}^n + c\mathbf{D}\mathbf{p}^n = \mathbf{0} \quad . \tag{46b}$$

Here, when combined with (45), a time-aligned scheme results, where all variables are calculated at multiples of the sample period k, and are indexed by integer n.

Another is to make use of a time-interleaved scheme (such schemes are typical in the electromagnetics literature[7,40]). Here, the scheme will operate over the discrete time-interleaved vectors $\mathbf{p}^n$ and $\mathbf{v}^{n+\frac{1}{2}}$, as well as the auxiliary boundary variables $(\mathbf{v}')^n$ and $(\mathbf{p}')^n$:

$$\delta_+ \mathbf{p}^n - c\mathbf{D}^T \mathbf{v}^{n+\frac{1}{2}} + c\mu_+ \mathbf{B}^T (\mathbf{v}')^n = \mathbf{0} \tag{47a}$$

$$\delta_- \mathbf{v}^{n+\frac{1}{2}} + c\mathbf{D}\mathbf{p}^n = \mathbf{0} \quad . \tag{47b}$$

Many other choices are of course possible, but the two above serve to illustrate important features common to all time-stepping methods for this system.

It is useful to note that in practice, second order forms are used in order to eliminate the variable $\mathbf{v}$ and compute solutions directly in terms of $\mathbf{p}^n$. Applying δ_- to (47a), for example, leads to the scheme

$$\delta_+\delta_- \mathbf{p}^n + c^2 \mathbf{D}^T \mathbf{D}\mathbf{p}^n + c\mu_+\delta_- \mathbf{B}^T (\mathbf{v}')^n = \mathbf{0} \tag{48}$$

which is a more familiar two-step update for $\mathbf{p}^n$, coupled to (45). (48) solves the 3D wave equation (16) directly. For analysis purposes, it is simpler to examine first-order schemes such as (47), and the equivalent two-step forms will not be discussed further in this article.

C. Implementation

Consider the first of (45), expressing a relationship between the time series $\left(v_b'\right)^n$ and $\left(p_b'\right)^n$, the normal velocity and pressure at boundary face b, $b = 1, \ldots, N_b$. Through the explicit expansion of the operators $\delta_\circ$, from (43), it may be written, ultimately, as a recursion

$$\left(v_b'\right)^{n+1} = \gamma_b \left(p_b'\right)^{n+1} + q_b^n \quad . \tag{49}$$

Here, γ_b is a constant derived from k, $\xi_b^{(\nu)}$, $\nu = 1, \ldots, M_b$ and $\eta_b^{(\nu)}$, $\nu = 1, \ldots, D_b$, and is constrained to be non-negative by the positive realness constraint on the associated admittance. q_b^n is a linear combination of previously computed values of $\left(v_b'\right)^m$ and $\left(p_b'\right)^m$, $n - \max(M_b, D_d) \leq m \leq n$. The values $\left(v_b'\right)^{n+1}$ and $\left(p_b'\right)^{n+1}$ are as yet unknown. In vector notation, using the second of (45),

$$(\mathbf{v}')^{n+1} = \mathbf{\Gamma}\mathbf{B}\mathbf{p}^{n+1} + \mathbf{q}^n \quad , \tag{50}$$

where $\mathbf{\Gamma}$ is a diagonal $N_b \times N_b$ matrix with γ_b, $b = 1, \ldots, N_b$ on the diagonal, and $\mathbf{q}^n$ is the $N_b \times 1$ column vector consisting of the values q_b^n, $b = 1, \ldots, N_b$.

Consider now the scheme (46), where it is assumed that all values $\mathbf{p}^n$, $\mathbf{v}^n$, and $(\mathbf{v}')^n$ are known up through time step n. Expanding the operator $\delta_\circ$ leads to

$$\mathbf{p}^{n+1} - \mathbf{p}^n - \frac{ck}{2}\mathbf{D}^T \left(\mathbf{v}^{n+1} + \mathbf{v}^n\right) + \frac{ck}{2}\mathbf{B}^T \left((\mathbf{v}')^{n+1} + (\mathbf{v}')^n\right) = \mathbf{0} \tag{51a}$$

$$\mathbf{v}^{n+1} - \mathbf{v}^n + \frac{ck}{2}\mathbf{D}\left(\mathbf{p}^{n+1} + \mathbf{p}^n\right) = \mathbf{0} \quad . \tag{51b}$$

Using (50), and consolidating the unknowns $\mathbf{p}^{n+1}$ and $\mathbf{v}^{n+1}$ into the column vector $\mathbf{y}^{n+1} = [\left(\mathbf{p}^{n+1}\right)^T \left(\mathbf{v}^{n+1}\right)^T]^T$ leads to the update

$$\mathbf{A}\mathbf{y}^{n+1} = \mathbf{N}\mathbf{y}^n + \mathbf{b}^n \quad , \tag{52}$$

where

$$\mathbf{A} = \begin{bmatrix} \mathbf{I}_N + \frac{ck}{2}\mathbf{B}^T\mathbf{\Gamma}\mathbf{B} & -\frac{ck}{2}\mathbf{D}^T \\ \frac{ck}{2}\mathbf{D} & \mathbf{I}_{N_e} \end{bmatrix} \tag{53}$$

and

$$\mathbf{N} = \begin{bmatrix} \mathbf{I}_N & \frac{ck}{2}\mathbf{D}^T \\ -\frac{ck}{2}\mathbf{D} & \mathbf{I}_{N_e} \end{bmatrix} \qquad \mathbf{b}^n = \begin{bmatrix} -\frac{ck}{2}\mathbf{B}^T \left(\mathbf{q}^n + (\mathbf{v}')^n\right) \\ \mathbf{0} \end{bmatrix} \quad . \tag{54}$$

This is an implicit numerical method, requiring the solution to a linear system involving the matrix $\mathbf{A}$ (which is positive definite, and thus a unique solution exists). Once $\mathbf{y}^{n+1}$ is determined, (50) may be used to solve explicitly for $(\mathbf{v}')^{n+1}$, and the entire procedure may be repeated.

Consider now the scheme (47), and assume that $\mathbf{p}^n$ and $(\mathbf{v}')^n$ are known through time step n, and $\mathbf{v}^{n-\frac{1}{2}}$ is known. The interleaving of $\mathbf{p}^n$ and $\mathbf{v}^{n+\frac{1}{2}}$ implies an alternating sequence of operations. First, (47b) may be expanded to yield an explicit update for $\mathbf{v}^{n+\frac{1}{2}}$ as

$$\mathbf{v}^{n+\frac{1}{2}} = \mathbf{v}^{n-\frac{1}{2}} - ck\mathbf{D}\mathbf{p}^n \quad . \tag{55}$$

Given $\mathbf{v}^{n+\frac{1}{2}}$, (47a) may be written as

$$\mathbf{p}^{n+1} = \mathbf{p}^n + ck\mathbf{D}^T\mathbf{v}^{n+\frac{1}{2}} + \frac{ck}{2}\mathbf{B}^T\left(\left(\mathbf{v}'\right)^{n+1} + \left(\mathbf{v}'\right)^n\right) \quad . \tag{56}$$

Using (50) one arrives, ultimately, at the update

$$\underbrace{\left(\mathbf{I}_N + \frac{ck}{2}\mathbf{B}^T\mathbf{\Gamma}\mathbf{B}\right)}_{\mathbf{\Theta}}\mathbf{p}^{n+1} = \mathbf{r}^n \quad , \tag{57}$$

where $\mathbf{r}^n$ consists of previously computed values.

This update appears to require a full linear system solution in order to solve for $\mathbf{p}^{n+1}$, using the matrix $\mathbf{\Theta}$ as defined in (57). Note first that the matrix $\mathbf{B}^T\mathbf{\Gamma}\mathbf{B}$ is sparse, and only affects the pressure update for cells which possess a boundary face; at all internal cells, the update can be explicitly computed. Furthermore, $\mathbf{B}^T\mathbf{\Gamma}\mathbf{B}$ is diagonal, and thus the solution of (57) requires merely multiplication by the inverse of $\mathbf{\Theta}$, which can be trivially precomputed. Thus, despite the use of an implicit discretisation method (the trapezoid rule) over the boundary, the entire update remains fully explicit. This explicit character (via the diagonal property of $\mathbf{B}^T\mathbf{\Gamma}\mathbf{B}$) is, however, dependent on the use of a locally reactive admittance model—that is, there is no interaction between the boundary faces adjoined to distinct cells.

D. Frequency Domain

In analogy with the continuous time case, for the analysis of time-stepping methods simulating a linear and time-invariant continuous-time system of ordinary differential equations, frequency domain analysis techniques are a useful tool. Full z-transform analysis is the most general approach, but as before, the use of an *ansatz* is entirely equivalent. In this case, consider solutions of the form

$$\mathbf{w}^n = \hat{\mathbf{w}}e^{s_d nk} \quad . \tag{58}$$

Here again, $\mathbf{w}^n$ could represent an approximation to any of the vectors $\mathbf{p}$, $\mathbf{v}$, $\mathbf{p}'$ or $\mathbf{v}'$ which appear in system (31) and (32). $\hat{\mathbf{w}} = \hat{\mathbf{w}}(s_d)$ is the complex amplitude, and $s_d = \sigma_d + j\omega_d$ is the discrete time complex frequency variable. By sampling considerations for discrete time systems, ω_d is limited to $-\pi/k < \omega_d \leq \pi/k$; thus values of s_d are limited to an infinite strip in the complex plane.

The various operators defined in Section V A when applied to the *ansatz*, can be viewed as multiplicative factors. For example,

$$\delta_+ \to e^{s_d k/2}\zeta_c \qquad \delta_- \to e^{-s_d k/2}\zeta_c \qquad \delta_\circ \to \zeta_\circ \quad , \tag{59}$$

where

$$\zeta_c(s_d) = \frac{2}{k}\sinh(s_d k/2) \qquad \zeta_\circ(s_d) = \frac{2}{k}\tanh(s_d k/2) \quad . \tag{60}$$

The special form of the function $\zeta_\circ(s_d)$, when viewed as a mapping between two complex variables $\zeta_\circ$ and s_d, is often referred to as the bilinear transformation; it is a one-to-one mapping between an infinite strip in the s_d plane and the entire $\zeta_\circ$ plane. In particular,

$$\mathrm{Re}(\zeta_\circ) \begin{matrix} > \\ = \\ < \end{matrix} 0 \qquad \Longleftrightarrow \qquad \mathrm{Re}(s_d) \begin{matrix} > \\ = \\ < \end{matrix} 0 \quad . \tag{61}$$

Similarly, the averaging operators μ_+ and μ_- behave as multiplicative factors

$$\mu_+ \to e^{\frac{s_d k}{2}}m_c \quad \mu_- \to e^{-\frac{s_d k}{2}}m_c \quad m_c(s_d) = \cosh(s_d k/2) \tag{62}$$

and note that $\zeta_\circ = \zeta_c/m_c$.

E. Stability Analysis

The general approach to the determination of stability conditions for numerical schemes such as (46) and (47) mirrors that of the continuous case. Assuming that all discrete time variables exhibit complex exponential time dependence, of frequency s_d as per the *ansatz* (58), conditions are sought such that all solutions satisfy $\mathrm{Re}(s_d) = \sigma_d \leq 0$ and are thus exponentially decaying.

The admittance relationship (32), is discretised uniformly using the approximation $d/dt \to \delta_\circ = (\mu_+)^{-1}\delta_+$ to yield (45). In the frequency domain, using (59), this leads to the discrete time admittance relationship

$$\hat{\mathbf{v}}' = \mathbf{Y}(\zeta_\circ)\hat{\mathbf{p}}' = \mathbf{Y}\mathbf{B}\hat{\mathbf{p}} \quad , \tag{63}$$

where $\mathbf{Y}$ is an $N_b \times N_b$ diagonal matrix with diagonal entries $Y_b(\zeta_\circ)$, as defined in (35) with $\zeta_\circ$ in place of s.

Consider now the scheme given in (46). In this case, the discretisation is performed uniformly using $d/dt \to \delta_\circ$, and thus, in discrete time, the characteristic equation

$$\underbrace{\begin{bmatrix} \zeta_\circ\mathbf{I}_N + c\mathbf{B}^T\mathbf{Y}(\zeta_\circ)\mathbf{B} & -c\mathbf{D}^T \\ c\mathbf{D} & \zeta_\circ\mathbf{I}_{N_e} \end{bmatrix}}_{\mathbf{G}(\zeta_\circ)}\begin{bmatrix}\hat{\mathbf{p}}\\ \hat{\mathbf{v}}\end{bmatrix} = \begin{bmatrix}\mathbf{0}\\ \mathbf{0}\end{bmatrix} \tag{64}$$

results. In this case, stability analysis follows directly from the continuous time case. Following from the results in Section IV G, the system possesses no solutions with $\mathrm{Re}(\zeta_\circ) > 0$. It then follows, from the passivity-preserving property of the bilinear transformation from (61), that there are no solutions for $\mathrm{Re}(s_d) = \sigma_d > 0$. This scheme is thus unconditionally stable.

Stability analysis for the scheme (47) is more delicate. Using $\mathbf{p}^n = \hat{p}e^{s_d nk}$ and $\mathbf{v}^{n+\frac{1}{2}} = \hat{v}e^{s_d nk}e^{s_d k/2}$ (note the additional nonzero factor of $e^{s_d k/2}$ reflecting the half time-step advance of $\mathbf{v}^{n+\frac{1}{2}}$ with respect to $\mathbf{p}^n$), the following characteristic equation results:

$$\underbrace{\begin{bmatrix} e^{\frac{s_d k}{2}}\zeta_c\mathbf{I}_N + ce^{\frac{s_d k}{2}}m_c\mathbf{B}^T\mathbf{Y}(\zeta_\circ)\mathbf{B} & -ce^{\frac{s_d k}{2}}\mathbf{D}^T \\ c\mathbf{D} & \zeta_c\mathbf{I}_{N_e} \end{bmatrix}}_{\mathbf{G}(s_d)}\begin{bmatrix}\hat{\mathbf{p}}\\ \hat{\mathbf{v}}\end{bmatrix} = \begin{bmatrix}\mathbf{0}\\ \mathbf{0}\end{bmatrix} \quad . \tag{65}$$

Again, assume that there exists a solution $s_d = \bar{s}_d = \bar{\sigma}_d + j\bar{\omega}_d$ with $\det(\mathbf{G}(\bar{s}_d)) = 0$, and where $\mathrm{Re}(\bar{s}_d) =$

$\bar{\sigma}_d > 0$. Under this condition, $\bar{m}_c = m_c(\bar{s}_d) \neq 0$ and $\bar{\zeta}_c = \zeta_c(\bar{s}_d) \neq 0$. It then follows that, for any nonsingular square $(N+N_e)\times(N+N_e)$ matrix $\mathbf{\Lambda}$, $\det(\mathbf{H}(\bar{s}_d)) = 0$ where $\mathbf{G} = \mathbf{\Lambda}\mathbf{H}$. Using the direct sum $\mathbf{\Lambda} = \left(e^{\frac{\bar{s}_d k}{2}}\bar{m}_c\right)\mathbf{I}_N \oplus \mathbf{I}_{N_e}$ leads to

$$\mathbf{H}(\bar{s}_d) = \begin{bmatrix} \bar{\zeta}_\circ \mathbf{I}_N + c\mathbf{B}^T\mathbf{Y}\left(\bar{\zeta}_\circ\right)\mathbf{B} & -\frac{c}{\bar{m}_c}\mathbf{D}^T \\ c\mathbf{D} & \bar{\zeta}_c\mathbf{I}_{N_e} \end{bmatrix} \quad . \tag{66}$$

The condition $\det(\mathbf{H}(\bar{s}_d)) = 0$ is equivalent to $\det(\mathbf{H}_{22}(\bar{s}_d))\det\left(\mathbf{H}_{22}^{SC}(\bar{s}_d)\right) = 0$ where, as in the continuous case, $\mathbf{H}_{22} = \bar{\zeta}_c\mathbf{I}_{N_e}$ is the lower $N_e \times N_e$ block of $\mathbf{H}$ (which is clearly nonsingular), and its Schur complement $\mathbf{H}_{22}^{SC}$ is defined by

$$\mathbf{H}_{22}^{SC} = \bar{\zeta}_\circ \mathbf{I}_N + c\mathbf{B}^T\mathbf{Y}\left(\bar{\zeta}_\circ\right)\mathbf{B} + \frac{c^2}{\bar{m}_c\bar{\zeta}_c}\mathbf{D}^T\mathbf{D} \quad . \tag{67}$$

Thus $\det\left(\mathbf{H}_{22}^{SC}\right) = 0$. This implies that there is a nonzero $N\times 1$ column vector $\mathbf{x}$ such that $\mathbf{x}^*\mathbf{H}_{22}^{SC}\mathbf{x} = 0$, where $\mathbf{x}^*$ is the conjugate transpose of $\mathbf{x}$. But, defining $\mathbf{w} = \mathbf{B}\mathbf{x}$,

$$\mathbf{x}^*\mathbf{H}_{22}^{SC}\mathbf{x} = \bar{\zeta}_\circ|\mathbf{x}|^2 + c\mathbf{w}^*\mathbf{Y}\left(\bar{\zeta}_\circ\right)\mathbf{w} + \frac{c^2}{\bar{m}_c\bar{\zeta}_c}|\mathbf{D}\mathbf{x}|^2 \quad , \tag{68}$$

and thus

$$\begin{aligned}\mathrm{Re}\left(\mathbf{x}^*\mathbf{H}_{22}^{SC}\mathbf{x}\right) &= \mathrm{Re}\left(\bar{\zeta}_\circ|\mathbf{x}|^2 + \frac{c^2}{\bar{m}_c\bar{\zeta}_c}|\mathbf{D}\mathbf{x}|^2\right) \\ &\quad + \underbrace{\sum_{b=1}^{N_b} c|w_b|^2\mathrm{Re}\left(Y_b\left(\bar{\zeta}_\circ\right)\right)}_{\geq 0} \quad .\end{aligned} \tag{69}$$

Here, the term including the effects of the admittances at the boundary cell faces is non-negative due to the passivity-preserving nature of the mapping $\zeta_\circ(s_d)$. It then follows that

$$\mathrm{Re}\left(\mathbf{x}^*\mathbf{H}_{22}^{SC}\mathbf{x}\right) \geq \mathrm{Re}\left(\bar{\zeta}_\circ|\mathbf{x}|^2 + \frac{c^2}{\bar{m}_c\bar{\zeta}_c}|\mathbf{D}\mathbf{x}|^2\right) \quad . \tag{70}$$

Now, note that

$$\nu = \mathrm{Re}\left(\bar{\zeta}_\circ\right) = \frac{2}{k}\frac{\sinh(\bar{\sigma}_d k)}{\cosh(\bar{\sigma}_d k) + \cos(\bar{\omega}_d k)} > 0 \tag{71a}$$

$$\mathrm{Re}\left(\frac{1}{\bar{m}_c\bar{\zeta}_c}\right) = \nu\frac{k^2}{2}\underbrace{\frac{\cos(\bar{\omega}_d k)}{\cosh(\bar{\sigma}_d k) - \cos(\bar{\omega}_d k)}}_{\Xi(\bar{s}_d)} \quad , \tag{71b}$$

and thus

$$\mathrm{Re}\left(\mathbf{x}^*\mathbf{H}_{22}^{SC}\mathbf{x}\right) \geq \nu\left(|\mathbf{x}|^2 + \frac{c^2k^2}{2}\Xi(\bar{s}_d)|\mathbf{D}\mathbf{x}|^2\right) \quad . \tag{72}$$

For $\bar{\omega}_d$ with $-\pi/2k \leq \bar{\omega}_d \leq \pi/2k$, $\Xi \geq 0$, and thus

$$\mathrm{Re}\left(\mathbf{x}^*\mathbf{H}_{22}^{SC}\mathbf{x}\right) \geq \nu|\mathbf{x}|^2 > 0 \quad . \tag{73}$$

For frequencies $\bar{\omega}_d$ with $\pi/2k < |\bar{\omega}_d| \leq \pi/k$, $\Xi < 0$, one may make use of the following bound:

$$|\mathbf{D}\mathbf{x}|^2 \leq \lambda_{\max}|\mathbf{x}|^2 \quad , \tag{74}$$

where $\lambda_{\max} > 0$ is the largest eigenvalue of the positive semidefinite matrix $\mathbf{D}^T\mathbf{D}$, to arrive at

$$\mathrm{Re}\left(\mathbf{x}^*\mathbf{H}_{22}^{SC}\mathbf{x}\right) \geq \nu\left(1 + \frac{c^2k^2}{2}\Xi\lambda_{\max}\right)|\mathbf{x}|^2 \quad . \tag{75}$$

For a given arrangement of cells, $\lambda_{\max}$ can be computed efficiently using various procedures, such as the Arnoldi algorithm[41].

Under the condition

$$k \leq \frac{2}{\sqrt{\lambda_{\max}}c} \quad , \tag{76}$$

one then has

$$\mathrm{Re}\left(\mathbf{x}^*\mathbf{H}_{22}^{SC}\mathbf{x}\right) \geq \nu(1 + 2\Xi)|\mathbf{x}|^2 \tag{77}$$

and, using the fact that $\Xi(\bar{s}_d) > -\frac{1}{2}$ when $\bar{\sigma}_d > 0$, one has, finally,

$$\mathrm{Re}\left(\mathbf{x}^*\mathbf{H}_{22}^{SC}\mathbf{x}\right) > 0 \quad . \tag{78}$$

Thus, under the condition (76), solutions for the scheme (47) with exponential growth are ruled out. The condition (76) is typical of explicit schemes such as (47). It recovers familiar stability conditions obtained by other methods in simplified cases, such as the well-known Courant-Friedrichs-Lewy condition[42] for basic regular FDTD schemes for the 2D or 3D wave equation. For example, consider an infinite problem domain, with a regular tiling of cubic cells of side length h. Now, $V_l = h^3$, $S_e = h^2$ and $H_e = h$, and the operator $\mathbf{D}^T\mathbf{D}$ is the negative of the familiar seven-point Laplacian operator, with maximal eigenvalue $\lambda_{\max} = 12/h^2$. The condition (76) reduces to the familiar condition $ck/h \leq 1/\sqrt{3}$ obtained through von Neumann analysis. Here, however, stability conditions have been obtained without any further conditions on problem geometry, or on the wall admittance, provided that they are passive and have been discretised through the passivity-preserving discretisation rule.

VI. CONCLUDING REMARKS

The most general aim of this article has been to provide a theoretical basis for the construction of numerically stable time stepping schemes for room acoustics.

An important conclusion here is that, from a design perspective, and for the FVTD designs presented here, the modeling problem can be separated into two independent parts—that of (a) the design of a scheme for a given room acoustics problem under perfectly reflective (Neumann) wall conditions, and (b) that of a scheme modeling the behaviour of the wall. The analysis of numerical stability may be confined to the much simpler case of (a) above, and numerically stable designs for the complete system (a) + (b) follow, regardless of the room geometry or wall conditions, provided they are passive.

The schemes described here were derived using the finite volume formalism. As mentioned elsewhere in this article, such schemes include many standard FDTD schemes as special cases, and in particular the popular nearest-neighbour schemes (such as that employing

a seven-point Laplacian, as mentioned in Section V E). There are many other varieties of schemes, however, for which the association with finite volume methods is less clear. These include methods where there is a trade-off between accuracy and locality, such as the many families of spectral[21] and higher-order accurate methods[43] for the 3D wave equation. One could envisage extending the analysis here to such schemes, where it could be expected from the analysis in Section V E, at least for two-step explicit methods, that stability conditions should depend only on the resulting Laplacian operator with homogeneous Neumann boundary conditions(which is effectively $-\mathbf{D}^T\mathbf{D}$). An advantage here, however, is that the discrete Laplacian arrived at using local finite volume approaches is negative semi-definite by construction—the proof in Section V E relies on this desirable attribute.

Only locally reactive wall conditions have been discussed in this article. This leads to some algorithmic simplification, particularly for the scheme (47) which remains fully explicit. No linear system solution is required for the update because there is no transmission of energy along the wall surface itself, which is reflected by the diagonal nature of the wall admittance matrix $\mathbf{Y}$. It is rather direct to see, however, from the compact form of the semi-discrete system given in (36), that the extension to the case of non-locally reactive boundary conditions could entail a generalisation of $\mathbf{Y}$ to a full symmetric matrix, perhaps with a sparsity pattern reflecting communication between neighboring boundary faces. If $\mathbf{Y}$ remains positive real, now in a matrix sense, then the bounds on pole locations for the complete system would follow as before. The schemes themselves would also have to be generalised, particularly with regard to the discrete-time admittance relationship (32), which will no longer decompose into a set of scalar discrete equations. Again, however, provided that $\mathbf{Y}$ remains positive real, and a passivity-preserving rule such as (59) is employed for the wall admittance relationships, then the conclusions regarding numerical stability in Section V E should continue to hold.

The results in this article hold in infinite precision arithmetic. In practice, however, rounding effects will be present, and instabilities may appear due to the "rounding" of a system pole to an unstable location, leading to "slow-growth" numerical instability. The onset of such instabilities generally depend on the number format (e.g., single or double floating point precision); see, e.g., the recent work[24]. Where it is desirable to use single precision in order to halve memory requirements over double precision, such as in large-scale room acoustics simulation, such onsets could appear prohibitively soon[44]. Resolving this potential difficulty of practical importance could warrant further study.

ACKNOWLEDGMENTS

This work was supported by the European Research Council, under grant numbers 2016-ERC-PoC-737574-WRAM and 2011-ERC-StG-279068-NESS. Thanks also for helpful comments from Danish Mohammed of the Birla University of Technology and Science.

[1] A. Krokstad, S. Strom, and S. Sørsdal, "Calculating the acoustical room response by the use of a ray tracing technique," J. Sound Vib. **8**(1), 118–125 (1968).

[2] J. Allen and D. Berkley, "Image method for efficiently simulating small-room acoustics," J. Acoust. Soc. Am. **66**(4), 943–950 (1979).

[3] A. Southern, D. Murphy, G. Campos, and P. Dias, "Finite difference room acoustic modelling on a general purpose graphics processing unit," in *Proc. 128th Audio Eng. Soc. Conv.*, London, UK (2010), paper 8028.

[4] J. Sheaffer and B. Fazenda, "FDTD/K-DWM simulation of 3D room acoustics on generalpurpose graphics hardware using compute unified device architecture (CUDA)," Proc. Inst. Acoust. **32**(5) (2010).

[5] B. Hamilton, C. J. Webb, N. D. Fletcher, and S. Bilbao, "Finite difference room acoustics simulation with general impedance boundaries and viscothermal losses in air: Parallel implementation on multiple GPUs," in *Proc. Int. Symp. Musical Room Acoust.*, Buenos Aires, Argentina (2016).

[6] Y. Yasuda and T. Sakuma, "Boundary element method," in *Computational Simulation in Architectural and Environmental Acoustics*, edited by T. Sakuma, S. Sakamoto, and T. Otsuru (Springer, 2014), p. 80.

[7] K. Yee, "Numerical solution of initial boundary value problems involving Maxwell's equations in isotropic media," IEEE Trans. Antennas Propagation **14**, 302–307 (1966).

[8] J. Virieux, "SH-wave propagation in heterogeneous media: velocity-stress finite-difference method," Geophysics **49**(11), 1933–1942 (1984).

[9] O. Chiba, T. Kashiwa, H. Shimoda, S. Kagami, and I. Fukai, "Analysis of sound fields in three dimensional space by the time-dependent finite-difference method based on the leap frog algorithm," J. Acoust. Soc. Japan **49**, 551–562 (1993).

[10] L. Savioja, T. Rinne, and T. Takala, "Simulation of room acoustics with a 3-D finite-difference mesh," in *Proc. Int. Comp. Music Conf.*, Århus, Denmark (1994), pp. 463–466.

[11] D. Botteldooren, "Acoustical finite-difference time-domain simulation in a quasi-cartesian grid," J. Acoust. Soc. Am. **95**(5), 2313–2319 (1994).

[12] L. Savioja, J. Backman, A. Järvinen, and T. Takala, "Waveguide mesh method for low-frequency simulation of room acoustics," in *Proc. 15th Int. Cong. Acoustics*, Trondheim, Norway (1995), pp. 637–640.

[13] D. Murphy, A. Kelloniemi, J. Mullen, and S. Shelley, "Acoustic modelling using the digital waveguide mesh," IEEE Sig. Proces. Mag. **24**(2), 55–66 (2007).

[14] K. Kowalczyk and M. van Walstijn, "Room acoustics simulation using 3-D compact explicit FDTD schemes," IEEE Trans. Audio Speech Language Proces. **19**(1), 34–46 (2011).

[15] B. Hamilton, "Finite difference and finite volume methods for wave-based modelling of room acoustics," Ph.D. thesis, University of Edinburgh, 2016.

[16] J. Saarelma, J. Botts, B. Hamilton, and L. Savioja, "Audibility of dispersion error in room acoustic finite-difference time-domain simulation as a function of simulation distance," J. Acoust. Soc. Am. **139**(4), 1822–1832 (2016).

[17] S. Bilbao, "Modeling of complex geometries and boundary conditions in finite difference/finite volume time domain room acoustics simulation," IEEE Trans. Audio Speech Language Proc. **21**(7), 1524–1533 (2013).

[18] S. Bilbao, B. Hamilton, J. Botts, and L. Savioja, "Finite volume time domain room acoustics simulation under general impedance boundary conditions," IEEE Trans. Audio Speech Language Proc. **24**(1), 161–173 (2016).

[19]J. Sheaffer, B. M. Fazenda, D. Murphy, and J. Angus, "A simple multiband approach for solving frequency dependent problems in numerical time domain methods," in *Proc. Forum Acusticum*, S. Hirzel (2011), pp. 269–274.

[20]N. Raghuvanshi, R. Narain, and M. C. Lin, "Efficient and accurate sound propagation using adaptive rectangular decomposition," IEEE Trans. Vis. and CG **15**(5), 789–801 (2009).

[21]M. Hornikx, W. De Roeck, and W. Desmet, "A multi-domain Fourier pseudospectral time-domain method for the linearized Euler equations," J. Comp. Phys. **231**(14), 4759–4774 (2012).

[22]R. Mehra, N. Raghuvanshi, L. Savioja, M. Lin, and D. Manocha, "An efficient GPU-based time domain solver for the acoustic wave equation," Appl. Acoust. **73**(2), 83–94 (2012).

[23]S. Bilbao, *Numerical Sound Synthesis: Finite Difference Schemes and Simulation in Musical Acoustics*, 140 (John Wiley and Sons, Chichester, UK, 2009).

[24]J. Botts and L. Savioja, "Spectral and pseudospectral properties of finite difference models used in audio and room acoustics," IEEE/ACM Trans. Audio, Speech, Language Proces. **22**(9), 1403–1412 (2014).

[25]S. Oxnard, "Investigating the stability of frequency-dependent locally reacting surface boundary conditions in numerical acoustic models," J. Acoust. Soc. Am. **143**(4), EL266–EL270 (2018).

[26]J. Strikwerda, *Finite Difference Schemes and Partial Differential Equations*, Chap. 2 (SIAM, Philadelphia, 2004).

[27]S. Osher, "Stability of difference approximations of dissipative type for mixed initial boundary value problems. I.," Math. Comp. **23**, 335–340 (1969).

[28]B. Gustafsson, H.-O. Kreiss, and A. Sundstrom, "Stability theory of difference approximations for mixed initial boundary value problems. II.," Math. Comp. **26**(119), 649–686 (1972).

[29]L. Trefethen, "Group velocity in finite difference schemes," SIAM Review **24**, 113–136 (1982).

[30]Y. H. J. Bin and S. Lee, "Broadband impedance boundary conditions for the simulation of sound propagation in the time domain," J. Acoust. Soc. Am. **125**(2), 664–675 (2009).

[31]K.-Y. Fung and H. Ju, "Impedance and its time-domain extensions," AIAA J. **38**(1), 30–38 (2000).

[32]E. Hairer, C. Lubich, and G. Wanner, *Geometric Numerical Integration: Structure-preserving Algorithms for Ordinary Differential Equations*, Vol. 31 (Springer Science & Business Media, 2006).

[33]S. Bilbao and B. Hamilton, "Passive time-domain numerical designs for room acoustics simulation," in *Proc. 22nd Int. Cong. Acoust.*, Buenos Aires, Argentina (2016).

[34]L. Weinberg, *Network Analysis and Synthesis*, 244 (R. E. Krieger, New York).

[35]A. Fettweis, "Wave digital filters: Theory and practice," Proc. IEEE **74**(2), 270–327 (1986).

[36]S. Bilbao and R. Harrison, "Passive time-domain numerical models of viscothermal wave propagation in acoustic tubes of variable cross section," J. Acoust. Soc. Am. **140**, 728–740 (2016).

[37]C. Desvages and S. Bilbao, "Two-polarisation physical model of bowed strings with nonlinear contact and friction forces, and application to gesture-based sound synthesis," Applied Sciences **6**, 1–32 (2016).

[38]P. Ioannou and G. Tao, "Frequency domain conditions for strictly positive real functions," IEEE Trans. Automatic Control **AC-22**(1), 53–54 (1987).

[39]R. Horn and C. Johnson, *Matrix Analysis*, 22 (Cambridge University Press, Cambridge, UK, 1990).

[40]A. Taflove, *Computational Electrodynamics* (Artech House, Boston, Massachusetts, 1995).

[41]R. B. Lehoucq, D. C. Sorensen, and C. Yang, *ARPACK Users' Guide: Solution of Large-scale Eigenvalue Problems with Implicitly Restarted Arnoldi Methods* (Siam, Philadelphia, 1998).

[42]R. Courant, K. Friedrichs, and H. Lewy, "Über die partiellen Differenzengleichungen de mathematischen Physik," Mathematische Annalen **100**, 32–74 (1928).

[43]S. Bilbao and B. Hamilton, "Higher order accurate two-step finite difference schemes for the many dimensional wave equation," J. Comp. Phys. **367**, 134–165 (2018).

[44]C. J. Webb and A. Gray, "Large-scale virtual acoustics simulation at audio rates using three dimensional finite difference time domain and multiple GPUs," in *Proc. Int. Cong. Acoust.*, Montréal, Canada (2013).